Geoderma 443 (2024) 116825

Contents lists available at ScienceDirect

Geoderma

journal homepage: www.elsevier.com/locate/geoderma

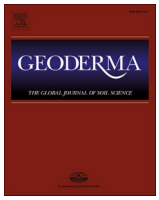

# Organic carbon stabilization in temperate paddy fields and adjacent semi-natural forests along a soil age gradient

Erik Schwarz [a], Anna Johansson [a], Cristina Lerda [b], John Livsey [a,c], Anna Scaini [a], Daniel Said-Pullicino [b], Stefano Manzoni [a,*]

[a] Department of Physical Geography and Bolin Centre for Climate Research, Stockholm University, Svante Arrhenius väg 8, SE-106 91 Stockholm, Sweden
[b] Department of Agricultural, Forest and Food Sciences, University of Torino, Largo Paolo Braccini 2, 10195 Grugliasco, Italy
[c] Department of Soil and Environment, Swedish University of Agricultural Science, Lennart Hjelms väg 9, SE-750 07 Uppsala, Sweden

ARTICLE INFO

Handling Editor: A. Agnelli

*Keywords:*
Mineral associated organic carbon
Particulate organic carbon
Fe oxyhydroxides
Rice paddy soil
Soil carbon storage

ABSTRACT

Rice paddy soils have high organic carbon (OC) storage potential, but predicting OC stocks in these soils is difficult due to the complex OC stabilization mechanisms under fluctuating redox conditions. Especially in temperate climates, these mechanisms remain understudied and comparisons to OC stocks under natural vegetation are scarce. Semi-natural forests could have similar or higher OC inputs than rice paddies, but in the latter mineralization under anoxic conditions and interactions between OC and redox-sensitive minerals (in particular Fe oxyhydroxides, hereafter referred to as Fe oxides) could promote OC stabilization. Moreover, management-induced soil redox cycling in rice paddies can interact with pre-existing pedogenetic differences of soils having different degrees of evolution. To disentangle these drivers of soil OC stocks, we focused on a soil age gradient in Northern Italy with a long (30 + years) history of rice cultivation and remnant semi-natural forests. Irrespective of soil age, soils under semi-natural forest and paddy land-use showed comparable OC stocks. While, in topsoil, stocks of crystalline Fe and short-ranged Fe and Al oxides did not differ between land-uses, under paddy management more OC was found in the mineral-associated fraction. This hints to a stronger redox-driven OC stabilization in the paddy topsoil compared to semi-natural forest soils that might compensate for the presumed lower OC inputs under rice cropping. Despite the higher clay contents over the whole profile and more crystalline pedogenetic Fe stocks in the topsoil in older soils, OC stocks were higher in the younger soils, in particular in the 50–70 cm layer, where short-range ordered pedogenetic oxides were also more abundant. These patterns might be explained by differences in hydrological flows responsible for the translocation of Fe and dissolved OC to the subsoil, preferentially in the younger, coarse-textured soils. Taken together, these results indicate the importance of the complex interplay between redox-cycling affected by paddy-management and soil-age related hydrological properties.

## 1. Introduction

Rice paddy fields cover a large area and are characterized by conditions promoting organic carbon (OC) stabilization. Therefore, paddy soils have a globally relevant carbon (C) storage potential (Liu et al., 2021). They are also net sources of greenhouse gases due to high emissions of methane and nitrous oxide, raising the question as to how their management can reduce emissions while preserving organic matter stocks (Bouman et al., 2007; Livsey et al., 2019). To this aim, we need to understand the pathways of OC stabilization in paddy soils, both in comparison to other land uses and agricultural management practices, and along pedoclimatic gradients.

Paddy soils generally accumulate more OC with respect to upland cropping systems both as a result of high crop residue inputs, especially in intensely managed areas where adequate fertilization promotes rice plant growth, and the maintenance of anoxic conditions for most of the rice growing season (Kögel-Knabner et al., 2010). Anoxic conditions reduce microbial activity because they require microbes to use electron acceptors that are energetically less favorable than oxygen, resulting in less efficient conversion of OC into biomass and overall slower decomposition rates compared to oxic conditions (Šantrůčková et al., 2004; Chakrawal et al., 2022). Different OC inputs between rice and other

* Corresponding author.
*E-mail address:* stefano.manzoni@natgeo.su.se (S. Manzoni).

https://doi.org/10.1016/j.geoderma.2024.116825
Received 24 February 2023; Received in revised form 9 February 2024; Accepted 17 February 2024
Available online 24 February 2024

vegetation types and reduced decomposition in paddy soils interact with redox processes affecting the dynamics and stabilization of OC.

C cycling in paddy fields is linked to redox cycling of iron (Fe) as Fe-containing minerals may both serve as alternative electron acceptors for OC mineralization under anoxic conditions and provide mineral surfaces for OC protection against microbial decomposition through chemical stabilization (Huang and Hall, 2017; Hall et al., 2018; Huang et al., 2020). The protection of OC that is associated with mineral surfaces (mineral-associated organic carbon, MAOC) from enzymatic attack makes this C pool functionally distinct from OC in particulate organic matter (particulate organic carbon, POC) that is more susceptible to decomposition (Lavallee et al., 2020; Cotrufo and Lavallee, 2022). Microbially-mediated Fe reduction under anoxic conditions can cause dissolution of Fe oxyhydroxides (hereafter referred to as Fe oxides), particularly of those having a low degree of crystalline order (Colombo et al., 2014). Thereby, $Fe^{II}$ is released into solution together with previously adsorbed OC that may be subsequently mineralized or leached into the subsoil (Said-Pullicino et al., 2016; Dunham-Cheatham et al., 2020). When oxic conditions are resumed, Fe precipitates, allowing for C adsorption and co-precipitation of C and Fe (Colombo et al., 2014; Mikutta et al., 2014; Said-Pullicino et al., 2016; Sodano et al., 2017). Dissolved Fe can migrate down the soil profile thanks to water percolation below the plough layer, which can cause a depletion of pedogenetic Fe oxides in paddy topsoils and a relative increase in the more crystalline Fe forms (Said-Pullicino et al., 2021). Simultaneously, illuvial Fe can accumulate in the subsoil, where it can be precipitated in oxidized form—primarily in the form of short-range ordered Fe oxides (Giannetta et al., 2022). Having large reactive surface areas, these less crystalline Fe oxides can stabilize relatively more OC than crystalline forms (Kleber et al., 2005), thereby providing a larger potential for OC stabilization, especially at depth (Said-Pullicino et al., 2021; Giannetta et al., 2022).

In addition to these physical–chemical processes, aggregate dynamics are also affected by land use (von Luetzow et al., 2008) and long-term flooding (Kögel-Knabner et al., 2010). Forest soils are expected to have a larger fraction of OC occluded in aggregates—which is thereby physically protected from microbial access—compared to agricultural soils. Permanent flooding causes even stronger aggregate breakdown compared to other soil managements, but formation of stable micro-aggregates (especially in subsoils) could promote OC stabilization (Giannetta et al., 2022).

As a result of the combination of these processes, paddy soils tend to store more C than nearby natural vegetation or other crops (Wu, 2011; Chiti et al., 2012; Liu et al., 2019). Yet, most studies focused on rice systems in tropical regions (where most of the rice-growing areas are located), with less attention devoted to temperate regions with a single cropping cycle per year. In these areas, flooded conditions are maintained for a relatively short period compared to tropical two or three crop systems, raising the question as to how much a single crop cycle per year can alter soil OC cycling compared to other land uses. Within temperate areas, paired paddy vs. non-paddy fields or paddy fields with different water management have been compared (Chiti et al., 2012; Said-Pullicino et al., 2016, 2021), but changes due to rice cultivation with respect to natural (or semi-natural) vegetation have not yet been investigated.

In addition to land use, soil age can also affect OC storage. In fact, shifts in the composition of soil mineralogy due to chemical weathering during pedogenesis strongly influence reactive mineral surface areas and consequently C storage due to the weathering of primary minerals to form secondary minerals including Fe oxides, Al oxyhydroxides and phyllosilicates (Wiesmeier et al., 2019). Moreover, these processes have been shown to be accelerated by periodic water saturation also resulting in substantial vertical differentiation in soil mineralogy and OC stabilization within the soil profile (Kölbl et al., 2014; Szalai et al., 2021).

Here we focus on north-west Italy (Vercelli province, Piedmont), where rice has been extensively cultivated since the 1860s. In the northern areas of Vercelli province, soils developed on sediments deposited between middle and upper Pleistocene and range from Alfisols on ancient terraces (medium Pleistocene) to Inceptisols on the river valley floors (upper Pleistocene or younger) (Regione Piemonte, 2022). The prolonged history of paddy soil management is expected to have profoundly impacted soil formation and consequently its physical and chemical properties (Kölbl et al., 2014). In the study area, remnant forested plots that have never been cultivated with rice offer an opportunity to evaluate soil changes caused by paddy cultivation along this soil age gradient. Compared to the younger, more productive soils in the lower Po Valley, the ancient soils in the northern Vercelli province are nutrient-poor. Despite this, we expect forested sites to produce equal or larger C inputs to soils compared to paddy fields. In fact, temperate forests in the same climate zone have total net primary productivity (as a proxy of the soil C input rate) of 400–1200 gC $m^{-2}$ $y^{-1}$ (Campioli et al., 2015; Nolè et al., 2015), whereas total C inputs in rice paddies with a single crop cycle per year are in the order of 400–500 gC $m^{-2}$ $y^{-1}$ (Said-Pullicino et al., 2016; Liu et al., 2019). However, OC stabilization is expected to be much less effective in the forest plots compared to the paddy fields.

Based on these premises, we address the following questions:

- How does OC storage differ between paddy soils and semi-natural vegetation along a soil age gradient under a temperate climate?
- What are the main processes contributing to OC stabilization when considering the interaction between land use and soil age—different distributions of OC pools along the profile or OC association with different pedogenetic Fe forms?

We hypothesized that:

H1: Although soils in semi-natural forests receive similar or higher OC inputs than soils used for rice cropping, redox-driven processes linked to paddy management can favour OC stabilization due to slow C mineralization under anoxic conditions and dynamic interactions with redox-active minerals, allowing paddy soils to accumulate similar or higher amounts of OC. We also expect OC to be distributed differently between soil fractions, with relatively more POC in the forest soils and more MAOC in the paddy soils.

H2: Redox-driven changes in Fe and C cycling along the soil profile in rice paddy soils depend on soil age. While in more evolved soils the greater contents of secondary minerals can be related to a higher capacity to stabilize OC by mineral association, in less evolved, more coarse-textured soils, higher leaching of C (and Fe) to the subsoil could cause larger C accumulation in the subsoil. We thus expect that soil age drives positive correlations in the deeper layers between less crystalline Fe and OC.

## 2. Methods

### 2.1. Study area

Paddy fields and relatively undisturbed forested plots have been identified around the municipality of Carisio (Vercelli province, Italy), in north-west Italy—at the northern edge of the largest rice growing area in Europe (Fig. 1). The selected area is characterized by alternating alluvial terraces of the medium Pleistocene era (elevation around 200 m above sea level) and younger fluvial deposits at lower elevation. The climate is warm temperate (mean annual temperature: 12.4 °C; mean annual precipitation: 932 mm; data from the meteorological station in Massazza, located 6–8 km north of the sampling sites and managed by the regional agency for environmental protection of Piedmont, ARPA Piemonte), with cool winters (monthly mean temperatures below 2.5 °C in December and January) and warm summers (above 20 °C from June to August). Precipitation is highest in May and November (above 100 mm per month), and lowest between December and March (less than 60 mm per month). During the summer, precipitation is highly variable and

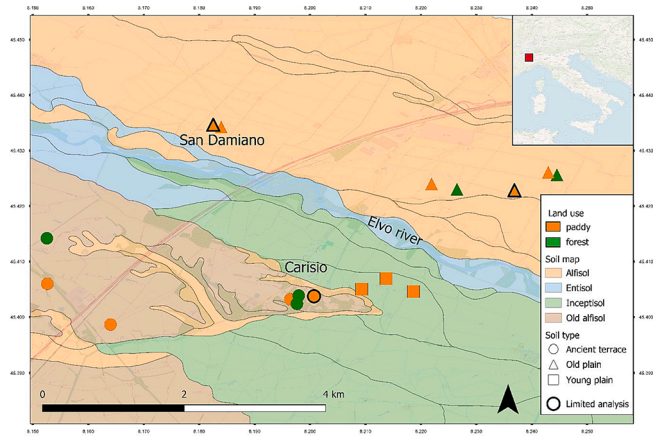


**Fig. 1.** Map of sampling sites overlaid on the soil map (elaborated after Regione Piemonte, 2022). Black outlines around symbols indicate sites with limited analysis (no organic matter density fractionation performed). The paddy soil on the ancient terrace marked by a black outline (circle) was removed from the statistical analyses (see details in Section 2.6).

concentrated in a few intense events.

In the study area, Inceptisols dominate on the river valley floors (upper Pleistocene or younger) while older Alfisols remain on ancient terraces (medium Pleistocene) (Regione Piemonte, 2022). This progression in a relatively small area with the same climatic conditions and topographic variations of approximately 20 m (180–200 m above sea level) allowed comparing soils with contrasting ages without confounding effects of climate and topography. These soils developed on fluvial sediments poor in carbonates, they are slightly acidic or neutral, and have loam to silty-loam texture; their organic matter content is expected to range from 20 to 40 g $kg^{-1}$ in the top 20 cm to approximately 5 g $kg^{-1}$ at 50 cm depth (see metadata in Regione Piemonte, 2022).

Rice (*Oryza sativa*) paddies dominate the landscape, with few fields cultivated with other crops or dedicated to tree plantations. Among the sampled fields, chemical NPK fertilizer is typically applied (seldom manure), and in some cases a winter cover crop (a mixture of *Lolium* sp. and *Trifolium* sp.) is sown in the autumn and incorporated into the soil as a green manure in the spring. Rice is either dry or water seeded depending on the farmers' practices and fields are drained 2–3 times per year for fertilizer and pesticide application. The average rice yield at the studies sites is around 7.3 t $ha^{-1}$ (range: 6–9 t $ha^{-1}$), with lower median values on the ancient terraces (6.5 t $ha^{-1}$) than in the plains (7 t $ha^{-1}$). The few remaining semi-natural forested areas besides the tree plantations are dominated by pedunculate oak (*Quercus robur*) or non-native black locust (*Robinia pseudoacacia*), but also include cherry trees (*Prunus avium*), poplars (*Populus* spp.), and European ash (*Fraxinus excelsior*). Understory woody species include *Rubus* and *Sambucus* spp., and limited herbaceous vegetation.

### 2.2. Units and definitions

Throughout the article, we refer to soil properties expressed as mass per unit soil dry weight (typically in units of mg $g^{-1}$) as 'contents', and to properties expressed as mass per unit soil volume (kg $m^{-3}$) as 'concentrations' (McNaught and Wilkinson, 1997). 'Stocks' are calculated as contents multiplied by soil bulk density ($\rho_b$) and sampling layer thickness, and are thus expressed as mass per unit ground area (kg $m^{-2}$ or t $m^{-2}$). Land cover categories are denoted as 'forest' and 'paddy'; soil types as 'ancient terrace' (AT), 'old plain' (OP), and 'young plain' (YP).

### 2.3. Soil sampling

Sampling was performed in October and November 2021, after rice harvest and before ploughing. We focused on three soil types with continuous paddy management for more than 30 years (as verified via interviews with farmers and 1986 aerial photographs from the Piedmont Region Web Map Service, https://www.geoportale.piemonte.it): Alfisols of the terraces (AT; labelled U309 in Regione Piemonte, 2022; medium Pleistocene), Alfisols of the plains (OP; labelled U493; medium to upper Pleistocene), and Inceptisols of the plains (YP; labelled U1020; upper Pleistocene) (Fig. 1).

Most fields had been leveled previously, but major leveling was mostly done 20–30 years ago. For two of these soil types (AT and OP), we also selected forested sites that had not been cleared for at least 20 years and have not been cultivated for at least 30 years (most important to this study, they have never been cultivated with rice). Those sites are considered in 'semi-natural' conditions in comparison with the heavily managed rice paddies, even though these are secondary-growth forests emerged from formerly cleared land, pastures or abandoned poplar plantations. In the following, we refer to these semi-natural forest sites simply as 'forest sites' for conciseness. At some of the forest sites, understory vegetation had been occasionally cleared in the previous years and we cannot exclude removal of some mature trees.

Depth profiles were sampled differently between paddy fields and forest sites to account for the different characteristics of the soil profiles. In paddy fields, we sampled layers of 0–20 cm, 20–30 cm (approximate location of the plough pan), 30–50 cm and 50–70 cm. At forest sites, after removing the little litter remaining at the end of the growing season, we sampled layers of 0–10 cm, 10–30 cm, 30–50 cm, 50–70 cm. This sampling allowed for capturing the sharp contrast between the organic matter rich uppermost soil layer (A horizons) and the deeper layers (B horizons), verified in representative soil pits, while maintaining the possibility of depth comparisons between soil types and land uses. Depth samples were successively taken with a soil auger. We followed a regular sampling scheme, with a central sampling point in the center of a paddy field or forest site and four perpendicular satellite samplings at ca. 10 m distance (protocol adapted from Livsey et al., 2021). A composite sample per depth layer was obtained by mixing the five replica soil cores from each site. Samples to calculate bulk density were taken at the central sampling point using a 100 $cm^3$ metal cylinder pushed horizontally into the soil at the center of each sampled layer.

As shown in Fig. 1, the numbers of replicate sites were 3 and 2 for forests on ancient terrace and old plain soils; 3, 5, and 3 for paddies on ancient terrace, old plain, and young plain soils, respectively. One paddy soil on the ancient terrace (marked by a black circle in Fig. 1) was regarded as outlier and not considered further in the statistical analyses due to its unusually low pH and high OC throughout the profile that suggested either significant disturbance during levelling or large inputs of organic matter in the past.

### 2.4. Physical soil properties

Oven-dried (100 °C, 12 h) soil from the 100 $cm^3$ samples was weighed to determine bulk density. Pebbles larger than 5 mm that were found in two samples were removed before weighing and the volume was corrected accordingly by removing the volume of the pebbles (calculated as pebble mass divided by density of 2.7 g $cm^{-3}$). Soil samples collected from the field were air-dried and ground to pass through a 2 mm sieve prior to analysis. A portion of the soil was further ground to pass through a 0.5 mm sieve. Soil pH was determined on a soil: water suspension (1:2.5 w/vol) of 2 mm-sieved air-dry soil.

The proportions of sand (2000 – 50 μm), silt (50 – 2 μm), and clay (<2.0 μm) were estimated by means of the hydrometer method following the procedure presented in Ashworth et al. (2001). In this methodology, the mass fractions of sand and clay particles are calculated based on their settling rate and the mass fraction of silt by difference.

### 2.5. Soil organic C and density fractionation

Soil organic matter density fractionation was performed on selected topsoils (0–30 cm depth): in all samples from the forest soils, but in only three replicates for each of the paddy soils (sites where no density fractionation was performed are marked by a black outline in Fig. 1). Density fractionation allowed separating the free particulate organic matter (fPOM), occluded particulate organic matter (oPOM), and mineral-associated organic matter (MOAM) (Golchin et al., 1994; Schmidt et al., 1999; Sohi et al., 2001; Moretti et al., 2020).

Briefly, 25 g of 2 mm-sieved, air-dried soil were suspended in 125 mL of sodium polytungstate (NaPT) solution (having a density of 1.6 g $cm^{-3}$). The suspension was gently mixed to ensure complete soil wetting while avoiding aggregate destruction and allowed to settle for about 30 min. The suspension was then centrifuged at 8500 rpm for 20 min. Floating and suspended organic matter in the supernatant was regarded as the fPOM fraction and was decanted on a 0.7 μm GF/F filter placed on a Buckner funnel with a vacuum pump running. The organic residue on the filter was washed with deionized water until the electrical conductivity of the filtrate was $< 20$ μS $cm^{-1}$.

The remaining soil was resuspended in 125 mL NaTP solution and ultrasonicated (Sonoplus HD 2200, Bandelin electronic GmbH & Co. KG, Berlin, Germany) applying an energy of 275 J $mL^{-1}$, avoiding dispersion of clay particles. The solution was centrifuged at 8500 rpm for 20 min. Floating and suspended organic matter in the supernatant was regarded as particulate organic matter previously occluded in soil aggregates (oPOM fraction) and was extracted in the same manner as fPOM.

The organic matter in the reminder of soil was regarded as the MAOM fraction. It was repeatedly washed with deionized water and centrifuged at 10000 rpm for 40–50 min until the conductivity of the supernatant was $< 50$ μS $cm^{-1}$.

All extracted fractions were dried in a ventilated oven at 40 °C, then weighted, ground to pass a 0.5 mm sieve and analyzed by high temperature combustion with an elemental analyzer (Unicube, Elementar, Germany) to determine the C and N contents. Inorganic C present in carbonate-containing soils was removed by acid treatment with HCl prior to elemental analysis.

### 2.6. Pedogenetic oxide contents

We assumed that in our small study area with soils developed on similar parent material, differences in pedogenetic Fe across sites are dominated by soil processes related to redox conditions and vegetation. Total pedogenetic Fe and short-range ordered (SRO) Fe and Al contents were determined on finely ground soil aliquots (<0.5 mm) by extraction with 0.3 M citrate-bicarbonate solution in the presence of sodium dithionite (DCB; denoted by $Fe_d$) and 0.2 M ammonium oxalate at pH 3 ($Fe_o$ and $Al_o$) as described by Mehra and Jackson (1960) and Schwertmann (1964), respectively. Fe and Al contents were determined by atomic absorbance spectroscopy (AAnalyst 400, Perkin Elmer). Crystalline oxides were estimated as the difference between $Fe_d$ and $Fe_o$ ($Fe_d$-$Fe_o$) and SRO oxides as the sum of $Fe_o$ and $Al_o$ ($Fe_o + Al_o$).

### 2.7. Statistical analyses

Two analyses were conducted: one focusing on data from paddy and forest sites on AT and OP soils, and one focusing on data from the paddy soils along the whole soil age gradient (AT, OP, YP). Univariate relations among soil properties were tested using Pearson correlation coefficients; multivariate relations were analyzed using linear mixed effect (LME) models. We analyzed separately contents along their depth profiles, and stocks distinguishing among total, topsoil (top two sampled layers, to a depth of 30 cm), and subsoil (two deeper layers: 30–50 and 50–70 cm depth) stocks. In all analyses, soil type and land use type were regarded as categorical variables. Information on rice yield and use of additional organic matter inputs (either through cover crops or organic amendments) was provided by the farmers during informal interviews. Both types of information were included as independent variables (the latter was regarded as a categorical presence/absence variable). OC contents showed a right-skewed distribution, so they were log-transformed prior to the statistical analyses.

In the analysis of depth profiles for soil chemical properties ($X$), we used a LME model with site as a random effect ($\delta$), and soil type ($S$), land use ($L$), and depth ($Z$) as fixed effects,

$$X_{i,j} = \alpha + \beta_S S_i + \beta_L L_i + \beta_Z Z_{i,j} + \delta_i + \epsilon_{ij} \quad (1)$$

where subscript $i$ refers to the site and $j$ to the depth (which is also site-dependent since sampling depths differed between forest and paddy soils); $\alpha$ is the intercept; $\beta$ are the regression coefficients of the fixed effects with subscripts referring to their respective independent variable; $\epsilon$ is the residual error. Interaction terms are not reported in Eq. (1) for conciseness, but are considered in the analysis. Density fractions (measured only in the first two top layers), were also predicted using the same model, but without interactions given the lower number of available datapoints. Because $S$ and $L$ are categorical variables, the estimated coefficients ($\beta_S$ and $\beta_L$, respectively) are the differences between $X$ values at a given $S$ or $L$ and the baseline values at $S = 0$ (AT soil) and $L = 0$ (forest). Equation (1) was applied to data from forest and paddy soils in AT and OP soils to test the effect of land use and soil type, and in a separate analysis on paddy soils only (including YP soils) to test the effect of soil type under paddy management (in this analysis, land use was removed from Eq. (1)).

In the stock ($\widehat{X}$) analysis, we first used a standard linear model similar to Eq. (1), but applied separately to the 0–30, 30–50, and 50–70 layers (i.e., depth was excluded),

$$\widehat{X}_{i,j} = \alpha + \beta_S S_i + \beta_L L_i + \epsilon_{ij} \quad (2)$$

Predicted variables were C stocks at the three depths $j$, and OC density fractions calculated as ratios of fPOC, oPOC, and MAOC stocks over OC stocks in the 0–30 cm layer. Equation (2) was applied (as Eq. (1)) to data from both land covers in AT and OP soils, and in a separate analysis on paddy soils only (including YP soils). No interactions were included in this model, because preliminary analysis showed they were not significant.

Using depth, land use, and soil age as predictors allows summarizing several factors driving soil properties into simpler categories. Moreover, these categories do not introduce collinearity issues that would emerge due to co-variation of several soil properties with depth. However, it is also useful to gain a more mechanistic insight on the effect of pedogenetic oxides and land use on C stocks and density fractions. To this aim, we adopted a LME model with crystalline Fe and SRO Fe and Al as fixed effects. This choice was motivated by soil minerals being stronger predictors of soil OC contents than other soil properties such as soil texture or pH (King et al., 2023). The resulting LME was,

$$\widehat{X}_i = \alpha + \beta_{d-o}(Fe_{di} - Fe_{oi}) + \beta_o(Fe_{oi} + Al_{oi}) + \delta_L + \epsilon_i \quad (3)$$

where crystalline Fe ($Fe_d$-$Fe_o$) and SRO Fe and Al ($Fe_o + Al_o$) stocks were used as fixed factors, while land use was treated as random factor ($\delta_L$), as a proxy to account for the effect of different C inputs and environmental conditions in forests and rice paddies.

Finally, we analyzed data from paddy soils only, removing the random factor from Eq. (3), but including rice yield ($Y_i$) as independent variable (presence of additional organic matter sources was tested but was not significant), resulting in the standard linear model,

$$\widehat{X}_i = \alpha + \beta_{d-o}(Fe_{di} - Fe_{oi}) + \beta_o(Fe_{oi} + Al_{oi}) + \beta_Y Y_i + \epsilon_i \quad (4)$$

Predictors were not normalized as their values (including binary 0 and 1 for $L$ and $S$) were within one order of magnitude. Therefore, the coefficients $\beta$ retain a physical meaning as the slopes of $\widehat{X}_i$ with respect to

the predictor, with units of $[\widehat{X}_i]/[\text{Predictor}]$.

All the data analyses were conducted in Matlab (The MathWorks Inc., 2018), using the functions *fitlme* and *fitlm* for linear mixed effect and standard models, respectively.

Differences are reported as significant when $p < 0.05$; in some cases, relevant trends that are only marginally significant or non-significant are mentioned, but always stating that they do not qualify as statistically significant.

## 3. Results

### 3.1. General patterns in soil properties

In all soils, clay fraction, bulk density, $Fe_d$ content, and percentage of MAOC increased with soil depth, whereas $Fe_o$ content, OC content, C:N ratio, and percentage of fPOC decreased (Figs. S2-S6). Comparing soils under different land uses (paddy-forest comparisons in Fig. S6), OC contents were not significantly different in general, though forest soils had higher topsoil OC contents (Fig. S3). However, the proportions of fPOC and oPOC were higher (and the proportion of MAOC was lower) in forest soil with respect to paddy soils (Fig. S5).

Comparing soils along the age gradient, clay (in particular at depth), $Fe_d$, and $Al_o$ contents generally increased, and $Fe_o$ generally decreased with increasing soil age as expected from the pedogenesis of these different soils (young to old: YP < OP < AT, Figs. S2, S4 and S6). $Fe_o$ was particularly high in the youngest soil at 20 to 70 cm depth (strong positive interaction of YP and depth in Fig. S6).

### 3.2. Land use and soil type effects on C stocks, density fractions and pedogenetic Fe stocks

OC stocks over the whole profile (0–70 cm) and OC stocks in most individual soil layers did not differ between land uses, but were higher in the OP compared to AT soils (analysis based on Eq. (2), Figs. 2 and 4). Despite similar overall OC stocks, paddy soils had lower OC stocks in the 50–70 cm layer than forest soils ($p < 0.1$). The percentages of oPOC and fPOC were lower and the percentage of MAOC was higher in the paddy soils compared to forest soils (Figs. 3 and 4). Moreover, the fractions of OC in oPOC and MAOC were significantly different between soil types, with lower MAOC and higher oPOC fractions in OP compared to AT soil (Figs. 3 and 4). Land use did not affect total pedogenetic Fe stocks over the whole profile, although paddy soils had slightly higher stocks of crystalline Fe phases in the deepest soil layers (Figs. 2 and 4).

When comparing paddy soils along the whole soil age gradient, clay stocks consistently increased with soil age (YP < OP < AT) (Figs. 2 and 5). Similarly, crystalline Fe stocks were higher in the older (AT and OP) compared to the younger (YP) soil over the whole profile and in most individual layers (Figs. 2 and 5). However, the stocks of less ordered $Fe_o$ and $Al_o$ phases were higher in the younger Inceptisols (YP) throughout the whole profile and especially in the subsoil, compared to the more evolved Alfisols (AT and OP) (Figs. 2 and 5). In subsoils (50–70 cm), OC was consistently higher in the lower elevation and younger soils (YP and OP) compared to AT (Figs. 2 and 5). The percentage of OC in the MAOC fraction in both YP and OP soils was lower than in the older AT soil (Figs. 3 and 5).

### 3.3. Relationships between pedogenetic oxides and OC across soil types and land uses

In univariate regressions, OC concentrations tended to decrease with increasing clay concentration across sites in all layers, but the relations were not significant (Fig. 6). Because clay and crystalline Fe oxide concentrations were positively correlated (Fig. S7), OC concentrations also tended to decrease with increasing concentration of crystalline Fe. This negative relation was significant only for paddy soils in the 30–50 cm layer (Fig. 6). OC concentration tended to decrease with increasing concentration of $Fe_o + Al_o$ in topsoils (though relations were not significant), but correlated positively in the deeper layers (only significantly for paddy soils in the 50–70 cm layer, Fig. 6). Overall, percentages of fPOC and oPOC decreased and percentages of MAOC increased with increasing concentration of clay, $Fe_d - Fe_o$, and $Fe_o + Al_o$ concentrations (only evaluated in the 0–30 cm layer), but these relations were statistically significant only in a few land use-density fraction combinations, and in particular for MAOC in forest soils (Fig. 7).

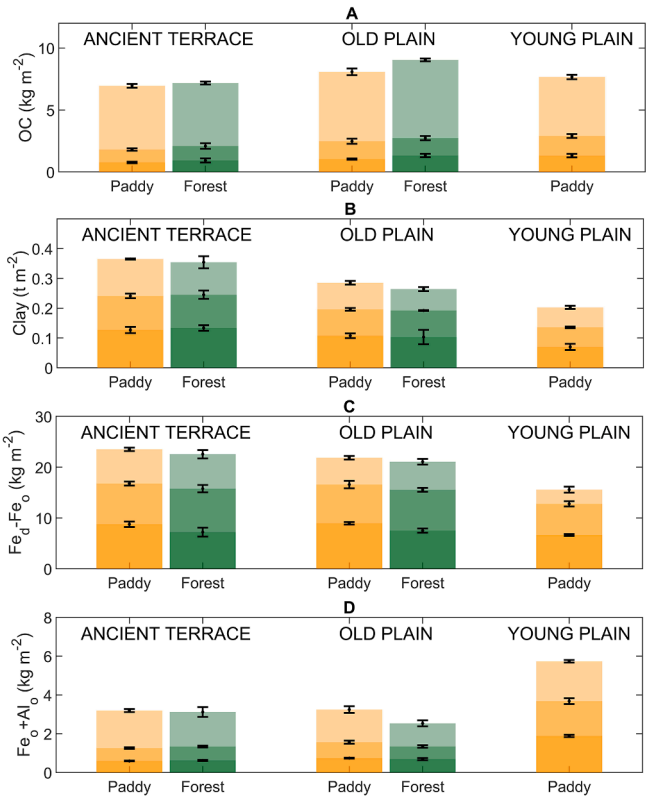


**Fig. 2.** Cumulative stocks of A) organic carbon (OC), B) clay, C) crystalline iron ($Fe_d$-$Fe_o$), and D) short-range ordered Fe and Al ($Fe_o + Al_o$). Shading becomes darker with increasing depth from 0–30 cm, to 30–50 cm and 50–70 cm. Error bars indicate mean and standard error for the stocks in the individual layers (n = 3, except n = 2 for ancient terrace forest soil and n = 5 for paddy old plain soil). Statistical differences among groups are reported in Fig. 4.

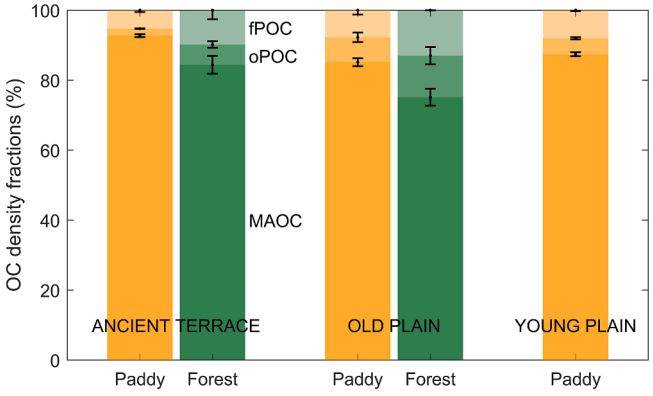


**Fig. 3.** Percentages of organic C (OC) in density fractions in the 0–30 cm layer. Shading becomes darker from free particulate OC (fPOC) to occluded particulate OC (oPOC) and to mineral-associated OC (MAOC). Error bars indicate mean and standard error for each density fraction (n = 3, except n = 2 for ancient terrace forest soil). Statistical differences among groups are reported in Fig. 4.

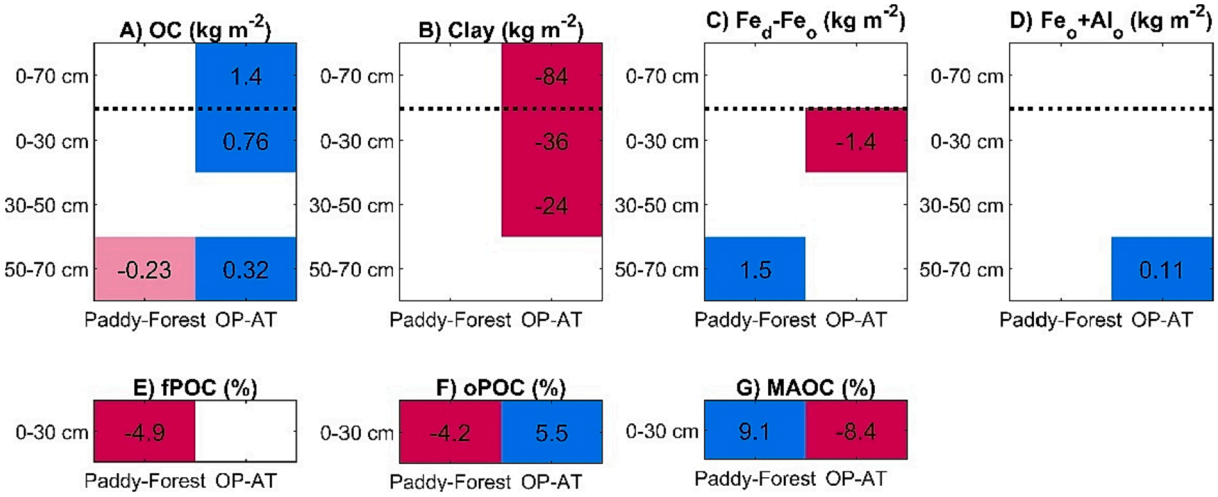


**Fig. 4.** Results of linear models (Eq. (2)) to predict from land use (paddy vs. forest) and soil type (AT: ancient terrace, OP: old plain) the stocks of: A) total OC, B) clay, C) crystalline Fe ($Fe_d$-$Fe_o$), D) short-range ordered Fe and Al ($Fe_o + Al_o$) at different depths; and E-G) OC density fractions in the 0–30 cm layer (fPOC: free particulate organic C, oPOC: occluded particulate organic C, MAOC: mineral associated organic C). Shading indicates the significance of the effect (blank: not significant, light colors: $0.05 < p < 0.1$, dark colors: $p < 0.05$). Colors indicate the direction of the effect (red: negative, blue: positive), and values are the estimated regression coefficients, reported only for the significant effects (Eq. (2)). Soil and land use are categorical variables, so coefficients represent differences compared to the baseline (forest and AT soil); e.g., 'Paddy-Forest' coefficients are differences between paddy and forest soils, 'OP-AT' coefficients are differences between OP and AT soils. Interactions are not included in the LME models for the density fractions.

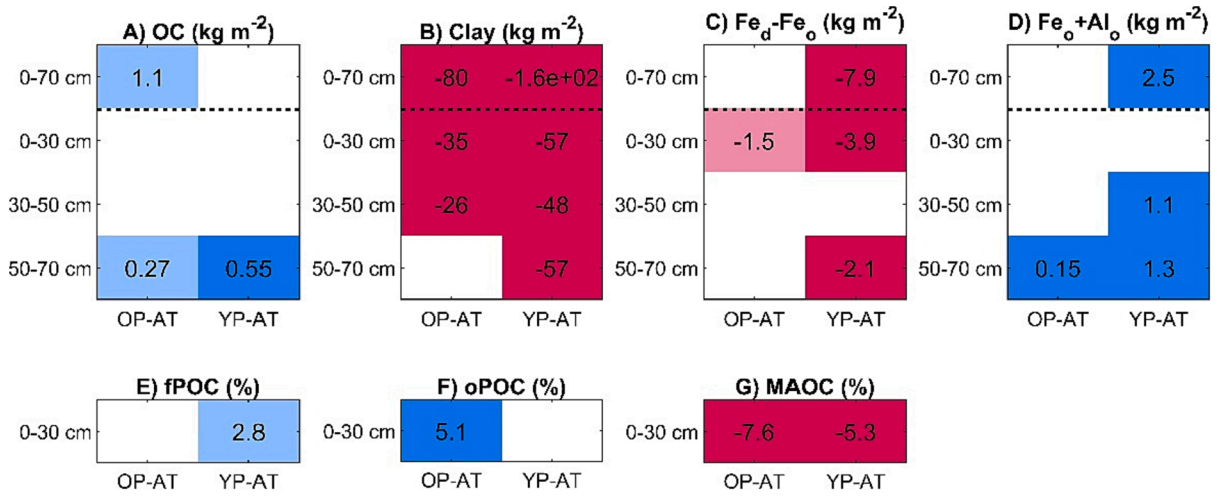


**Fig. 5.** Results of linear models (Eq. (2)) applied to rice fields only to predict from soil type (AT: ancient terrace, OP: old plain, YP: young plain) the stocks of: A) total OC, B) clay, C) crystalline Fe ($Fe_d$-$Fe_o$), D) short-range ordered Fe and Al ($Fe_o + Al_o$) at different depths; and E-G) OC density fractions in the 0–30 cm layer (fPOC: free particulate organic C, oPOC: occluded particulate organic C, MAOC: mineral associated organic C). Shading represents significance level and values are estimated differences between categories (see caption of Fig. 4).

These results based on univariate relations were generally confirmed by a linear model including both $Fe_d$-$Fe_o$ and $Fe_o + Al_o$ stocks as independent variables (Eq. (3), Fig. 8A). In this analysis, the percentages of MAOC significantly increased with both $Fe_d$-$Fe_o$ and $Fe_o + Al_o$, whereas both fPOC and oPOC significantly decreased with $Fe_o + Al_o$ (Fig. 8C-E). When focusing on paddy soils, a clear positive effect of rice yield (as a proxy of C inputs) on OC appeared in all layers (Eq. (4), Fig. 8B), overshadowing most of the negative effects of pedogenetic oxides on OC stocks shown in Fig. 8A.

## 4. Discussion

### 4.1. No differences between paddy and forest soil OC stocks

Total OC stocks observed in paddy soils were comparable to those reported in a recent study on paddy soils in an adjacent province in Northern Italy (8.1 kg $m^{-2}$ along the entire 100 cm deep profile) (Said-Pullicino et al., 2021) and stocks were similarly distributed between top- and subsoil (5.5 kg $m^{-2}$ and 2.6 kg $m^{-2}$ reported in top- (0–30 cm) and subsoils (30–100 cm) respectively by Said-Pullicino et al., 2021). In their study, Said-Pullicino et al. (2021) observed significantly larger OC stocks in paddy soils as compared to non-paddy (maize monoculture) soils, which was especially pronounced in the subsoil. Here we compared OC stocks in paddy soils not to soil under another arable crop, but to semi-natural forest soils. We do not have local estimates for the productivity of the sampled forests, but the net primary productivity (excluding rhizodeposits) of pedunculate oak forests in the same climate zone range between about 750 and 970 g C $m^{-2}$ $y^{-1}$ (Sever et al., 2019), comparable to temperate forests in general (Campioli et al., 2015). Estimates of net primary productivity from combined modelling, remote sensing, and plot data are ~ 400 g C $m^{-2}$ $y^{-1}$ for the 'deciduous mixed oak' vegetation class in Italy (Nolè et al., 2015). These different

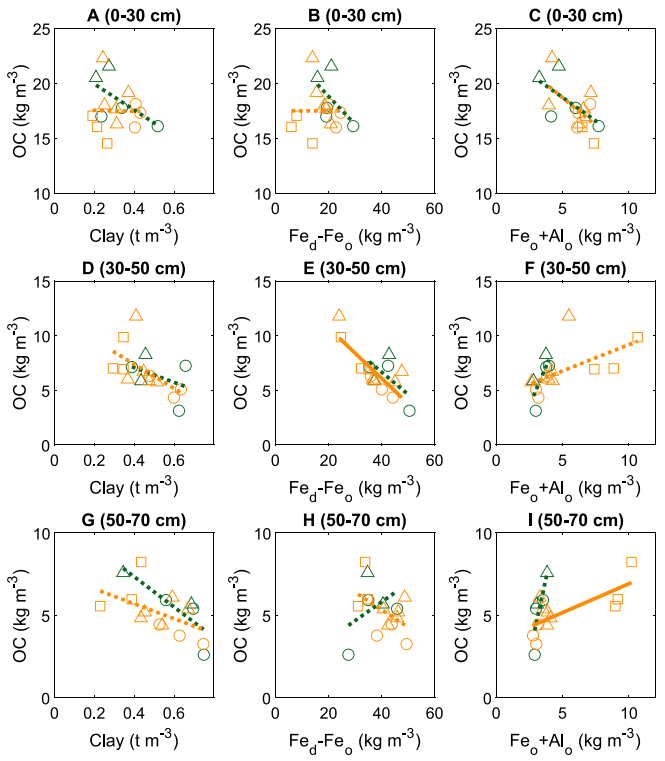


**Fig. 6.** Univariate relations between concentrations of organic carbon (OC) and clay (A, D, G), crystalline iron ($Fe_d$-$Fe_o$) (B, E, H), and short-range ordered Fe and Al ($Fe_o + Al_o$) (C, F, I), at different depths (increasing from top to bottom rows). Lines are linear regressions for paddy soils (orange) and forest soils (green); solid lines indicate slopes significantly different from zero ($p < 0.05$); symbols indicate soil types as in Fig. 1. Quantities are expressed as concentrations to allow comparisons between layers of different thickness.

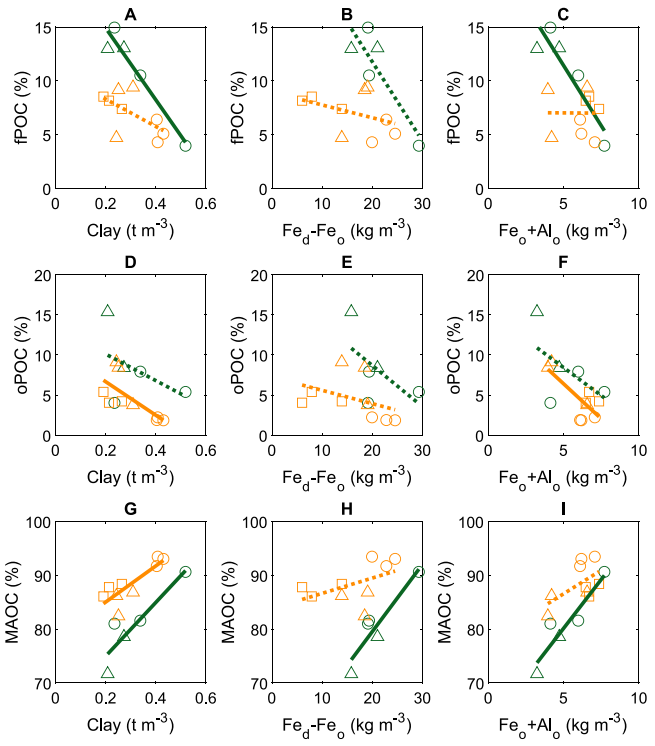


**Fig. 7.** Univariate relations between topsoil (0–30 cm) organic carbon (OC) fractions (from top to bottom: free particulate OC, fPOC; occluded particulate OC, oPOC; mineral-associated OC, MAOC) and concentrations of clay (A, D, G), crystalline iron ($Fe_d$-$Fe_o$) (B, E, H), and short-range ordered Fe and Al ($Fe_o + Al_o$) (C, F, I). Lines are linear regressions for paddy soils (orange) and forest soils (green); solid lines indicate slopes significantly different from zero ($p < 0.05$); symbols indicate soil types as in Fig. 1.

estimates give a wide productivity range for the climate zone of our study area. However, at our nutrient poor forest sites, some of which characterized by a partly open canopy, we expect productivities around the lower end of this range, thus similar or slightly higher than expected C inputs in the rice paddies. Our measurements indicate that, over the entire soil profile, forest soils had only slightly—but not significantly—higher total OC stocks than paddy soils despite comparable or higher C inputs and much lower soil disturbance, pointing to the OC stabilization potential of paddy soils.

Although we expected the particular hydraulic properties resulting from paddy management to favour the translocation of OC to greater soil depths (Said-Pullicino et al., 2016), paddy subsoils (50–70 cm depth) had slightly smaller OC stocks than forest subsoils (Figs. 2A and Fig. 4A). Characteristically, paddy soils are flooded for several consecutive months, which can increase leaching of dissolved and colloidal OC to the subsoil compared to other arable soils (e.g., under maize cultivation, Said-Pullicino et al., 2021), reaching fluxes of up to 33–51 g C $m^{-2}$ $y^{-1}$ (Said-Pullicino et al., 2016). Considering that the vertical distribution of OC we observed in paddy soils was similar to that observed by Said-Pullicino et al. (2021), leaching of OC below the plough pan was likely occurring in the paddy fields investigated here as well, despite their much higher clay content that could have limited water percolation. While the prolonged flooding of rice paddies distinguishes them from other arable crop soils, other processes might determine OC profiles in forest soils. For instance, forest soils lack a compacted plough pan and might have higher macroporosity compared to arable soils, allowing water to percolate unhindered (Messing et al., 1997). Moreover, roots of tree species reach deeper than crop roots (Jackson et al., 1996), thereby supplying larger C inputs at depth. These processes might explain the slightly higher OC stocks at depth in the forest sites.

Within the sites under paddy management, there was a significant positive correlation of OC stocks with rice yield (though yield values were based on the estimates provided by the farmers and not measured). This pattern is expected, as higher C inputs increase OC contents in croplands (King et al., 2023), but also because soils richer in organic matter are likely more productive thereby resulting in higher crop yields and consequently higher C inputs when crop residues are incorporated (Pan et al., 2009; Ma et al., 2023). This positive correlation between soil OC stocks and yields was consistent throughout the entire soil profile, suggesting that the additional C introduced into soils in productive fields can be stabilized by interactions with soil minerals and/or transported to and stabilized at depth. Additional influences of soil or crop management such as application of organic fertilizer and use of cover crops could not be rigorously tested as farmers could only provide anecdotal information of their management practices and hence it was not possible to estimate actual C input rates from these practices. We can speculate that increasing C inputs would promote additional C storage; in contrast, reducing the duration of field flooding (as a consequence of decreasing water availability or increasing adoption of water-saving practices) would be likely to reduce C stocks—albeit with the benefit of also reducing $CH_4$ emissions (Livsey et al., 2019).

### 4.2. *No differences between paddy and forest pedogenetic oxide stocks*

The larger accumulation of soil OC in soils under paddy management with respect to other upland arable soils has often been attributed to the direct effects of alternating redox conditions in promoting the formation of organo-mineral associations that contribute to the long-term stabilization of OC (Winkler et al., 2019). Consequently, we expected that the similar OC stocks in paddy and forest soils could be, to some extent, attributed to redox-induced differences in pedogenetic Fe mineralogy

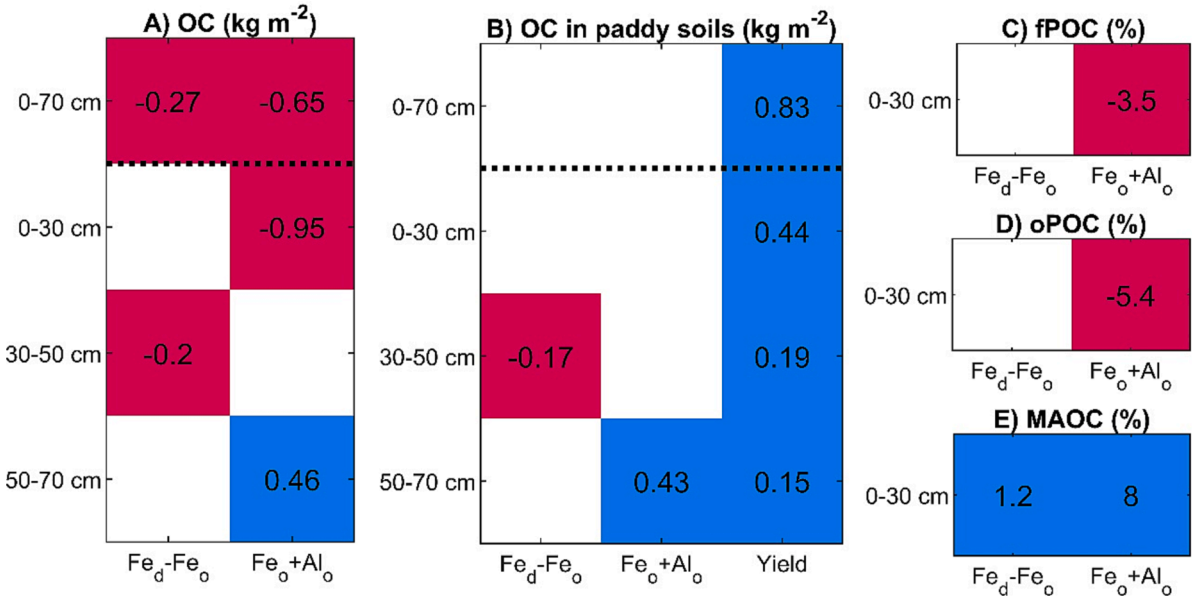


**Fig. 8.** Results of linear models (Eqs. (3) and (4)) with soil organic C (OC) stocks at different depths (A-B) and OC density fractions in the 0–30 cm layer (C-E) as dependent variables and crystalline iron ($Fe_d$-$Fe_o$), and short-range ordered Fe and Al ($Fe_o + Al_o$) stocks as independent variables (columns). In A and C-E, data from both land uses are included (Eq. (3)); in B, only data from paddy soils are used and rice yield is added as independent variable (Eq. (4)). Shading represents significance level and values are estimated coefficients of the statistical models for each of the independent variables (Eq. (3)-(4); see also caption of Fig. 4).

and depth distribution between land uses. In contrast to our expectation, there were no significant differences in the stocks of more crystalline ($Fe_d - Fe_o$) or the SRO ($Fe_o + Al_o$) metal oxides along the soil profiles under paddy and forest (Fig. 4). Alternating soil redox conditions during the cropping season in rice paddy fields together with the annual input of fresh crop residues, have been shown to deplete both SRO and more crystalline Fe phases in the topsoil and increase predominantly SRO oxides in the subsoil beneath the plough pan in relatively young, temperate rice paddies (Said-Pullicino et al., 2021). When compared to the dynamics in forest soils, the enhanced vertical translocation of metal oxides due to their reductive dissolution in the topsoil and their subsequent precipitation as SRO oxides in the subsoils with paddy management did not seem to be a dominant process in the older soils. Yet, these transport processes seem much more important in the younger paddy soil, for which we, however, do not have paired forest sites.

In the more evolved soils, the similar pedogenetic Fe stocks across land uses might be in part explained by the fact that any redox-induced changes in the degree of crystallinity and vertical distribution of these mineral phases may be masked by the relatively high amounts of total pedogenetic Fe present in these more evolved Alfisols. Compared to data from Said-Pullicino et al. (2021) for paddy soils developed on young plains (Inceptisols), the stocks of crystalline Fe oxides ($Fe_d$-$Fe_o$) in our paddy soils were distinctly higher in top- (3–6 fold) and subsoils (2–3 fold) and stocks of SRO Fe oxides ($Fe_o$) were similar in topsoils but distinctly (2–7 fold) lower in subsoils (though Said-Pullicino et al. (2021) sampled to a depth of 100 cm). An earlier study conducted on terraces along the Elvo River plain North of our study area (Arduino et al., 1986) reported similar contents of $Fe_d$ in old Alfisols (1.90–2.55 % in their study compared to 1.7–2.9 % in our study) with a consistent increase of $Fe_d$ contents with depth (Fig. S4). While $Fe_o$ contents in our ancient terrace topsoils compared well with the values found in their study, the subsoils in our study were comparably depleted in $Fe_o$ (ca. 0.1 % $Fe_o$ at 50–70 cm vs. 0.35 % at 56–92 cm in Arduino et al. (1986)). This depletion might be explained by less colloidal Fe leaching below the plough pan in these finer-textured soils (see Section 4.3 below), but the underlying mechanisms cannot be conclusively assessed with the available data.

### 4.3. Both OC and metal oxide stocks varied consistently with soil age

The significantly higher OC stocks in old plain (OP) with respect to ancient terrace (AT) soils over both land uses (Figs. 4A and Fig. 5A), as well as the consistent increase in paddy subsoil (50–70 cm) OC stocks from older to younger soils (Fig. 5A; results for the YP-OP comparison not shown), are in line with our expectation of OC, Fe, and Al leaching from topsoil and the simultaneous accrual of OC and SRO oxides in the subsoil (Said-Pullicino et al., 2016; 2021). In fact, the lower stocks of crystalline Fe minerals in topsoils and the larger stocks of SRO Fe and Al oxides in the subsoil of younger soils compared to older soils (Figs. 4 and 5) clearly indicate that depletion of pedogenic Fe from topsoil and consecutive accumulation of SRO Fe species in the subsoil was more pronounced in the less pedogenised soils. Increased pedogenic Fe contents in older soils could be a result of continued weathering of primary minerals, as also indicated by the higher clay fraction in older soils (Figs. 4 and 5). The higher clay content might also reduce the hydraulic conductivity of older soils and thus hinder the leaching of dissolved OC, Fe, and Al down the soil profile. This might explain both the lower OC and SRO mineral concentrations in the subsoil of older soils. Taken together, these results indicate that soil age—potentially via the associated differences in hydraulic properties—might play an important role in controlling OC and mineral distribution along the soil profile.

Moreover, OC stocks in subsoils increased with SRO oxide stocks. This is in line with our general expectations that SRO minerals might increase OC storage in soils due to their higher specific surface area (Said-Pullicino et al., 2021; Giannetta et al., 2022). This was further supported by the linear mixed effects model analysis using $Fe_o + Al_o$ stocks as a predictor for OC stocks (Fig. 8). In contrast to the deeper layer, correlations between $Fe_o + Al_o$ and OC stocks considering the entire profiles and in the shallower layers were negative (Fig. 8A). However, this unexpected negative relation disappeared when focusing on paddy soils and accounting for yield as an additional predictor (Fig. 8B). This supports our hypothesis of a positive correlation between OC and $Fe_o + Al_o$ stocks, but only at depth and after differences in C inputs to soil are also accounted for.

### 4.4. Short-range order minerals and land use influence the distribution of soil OC between functional pools

To place our results into context, MAOC stocks in the topsoils of our semi-natural forests were similar to the estimated average stocks in EU and UK broad-leaved forests (5.2 kg $m^{-2}$ in the 0–20 cm layer, Lugato et al. (2021)), but POC (fPOC + oPOC) stocks were considerably lower (0.8–1.6 kg $m^{-2}$ in our study compared to 2.7 kg $m^{-2}$ in the 0–20 cm layer in Lugato et al. (2021)), pointing to the expected low productivity of these forests growing on comparably poor soils. In paddy topsoils, MAOC stocks were slightly larger than the estimated average stocks in EU and UK arable soils (4.3 kg $m^{-2}$ in the 0–20 cm layer, Lugato et al. (2021)) and topsoil POC stocks were again considerably lower (0.4–0.9 kg $m^{-2}$ in our study vs. 1.8 kg $m^{-2}$ POC in 0–20 cm layer, Lugato et al. (2021)).

Both POC fractions (fPOC and oPOC) were significantly higher in forest than in paddy soils. This might be the result of the higher presence of structural constituents in the litter input (e.g., lignin) in forests compared to paddy fields, which leads to slower decomposition of POC. Not only fPOC, but also oPOC was higher in forest topsoils, suggesting that aggregation is stronger in forests, or aggregate stability is lower in paddy soils. In contrast, MAOC made up a significantly larger portion of total soil OC in paddy soils.

Regardless of soil age and land use, the portion of soil OC stabilized as MAOC in the topsoil was positively correlated to both crystalline and SRO oxide contents, indicating that adsorption to these species plays an important role in C stabilization—together with C inputs (King et al., 2023). This is in line with the idea that the dominating stabilization mechanism in slightly acidic soils (as our paddy and forest topsoils at ca. pH 6 and 5, respectively) might be adsorption to short-range ordered minerals and/or with Fe/Al organo-mineral complexes (Rasmussen et al., 2018). Since paddy and forest topsoil neither differed in their crystalline and SRO oxide contents nor their clay content, there is no obvious explanation available for the higher MAOC contents in paddy topsoils based only on these proxies. Several processes might be at play simultaneously and their balance might explain this pattern. Winkler et al. (2019) found that redox fluctuations can increase organo-mineral associations and the stabilization of rice straw-derived OC, though this effect may depend on soil mineral composition and was only observed in a soil with high $Fe_o$ concentrations in their experiments. Moreover, frequent redox fluctuations in rice paddies may promote C retention by co-precipitation rather than only by surface adsorption onto SRO Fe oxides, as the former was shown to result in a much higher C retention with important amounts of C included within highly aggregated Fe-OM associations (Sodano et al., 2017). Conversely, prolonged flooding in paddy soils causes reductive conditions and an increase in pH that can promote the release of adsorbed OC from soil minerals (Grybos et al., 2009; Said-Pullicino et al., 2016), which in turn might render it susceptible to microbial uptake or leaching to the subsoil, consequently depleting topsoil MAOC. Moreover, litter quality might play a role as crop residues (rice straw) are more easily degradable by microbes than more lignin-rich forest litter. This could lead to higher C stabilization via the *in vivo* pathway (thanks to increased microbial necromass) or the *ex vivo* pathway (stabilization of depolymerization products) (Liang et al., 2017).

## 5. Conclusions

We compared OC and pedogenetic oxide stocks in temperate paddy fields to those in semi-natural forests along a soil chronosequence. Soils under paddy management had similar total OC stocks with a higher proportion of mineral-associated OC with respect to forest soils. Yet, more OC was stored in forest subsoils than in paddy subsoils, suggesting an important role of hydrologic connectivity and deep roots for deep C storage in forests. In contrast, stabilization of OC in association with mineral oxyhydroxides appears to be the dominant mechanism of OC stabilization in the redox-dynamic paddy topsoils rather than a more pronounced leaching of OC and/or translocation of pedogenetic oxides to the subsoil. Nonetheless, younger paddy soils were comparably depleted in crystalline metal oxides in topsoils and had increased contents of less crystalline mineral phases in the subsoils, which were accompanied by increased subsoil OC stocks. This data supports our conceptual understanding of pedogenetic, redox-driven translocation of metal oxide phases from the topsoil and their consecutive precipitation in the subsoil as short-range order species. Our finding that total OC stocks are similar in semi-natural forest and paddy soils, but are differently distributed along the profile and among density fractions, points to the role of combined redox and hydrological processes to explain OC storage in paddy vs. semi-natural forest soils.

The complete dataset is available from the Bolin Centre Database (https://doi.org/10.17043/schwarz-2023-soil-1).

## CRediT authorship contribution statement

**Erik Schwarz:** Writing – review & editing, Writing – original draft, Methodology, Investigation, Formal analysis, Data curation, Conceptualization. **Anna Johansson:** Writing – review & editing, Investigation, Data curation. **Cristina Lerda:** Writing – review & editing, Methodology, Investigation, Data curation. **John Livsey:** Writing – review & editing, Investigation, Data curation, Conceptualization. **Anna Scaini:** Writing – review & editing, Investigation, Data curation, Visualization. **Daniel Said-Pullicino:** Writing – review & editing, Writing – original draft, Supervision, Methodology, Funding acquisition, Conceptualization. **Stefano Manzoni:** Writing – review & editing, Writing – original draft, Visualization, Supervision, Project administration, Methodology, Investigation, Funding acquisition, Formal analysis, Data curation, Conceptualization.

## Declaration of competing interest

The authors declare that they have no known competing financial interests or personal relationships that could have appeared to influence the work reported in this paper.

## Acknowledgements

We thank Thomas Kätterer for his valuable contribution in the initial planning phase and for subsequent discussions, and the land owners for allowing access to their fields and forested areas, and for providing information on the history and current practices of land management at the study sites. Three reviewers provided constructive comments. We also thank S. M. Zunino for hospitality and logistical support during the field campaign. ES and SM were supported by the European Research Council, under the European Union's Horizon 2020 research and innovation programme (grant no. 101001608); AJ, JL, and AS were supported by the Swedish Research Council (Vetenskapsrådet), Formas, and Sida through the joint call "Sustainability and resilience – Tackling climate and environmental changes" (VR 2016-06313); DSP was supported by the Agritech National Research Center related to Spoke 4 "Multifunctional and resilient agriculture and forestry systems for the mitigation of climate change risks" funded by the European Union Next-Generation EU (Piano Nazionale di Ripresa e Resilienza (PNRR) – Missione 4 Componente 2, Investimento 1.4 – D.D. 1032 17/06/2022, CN00000022). The funding sources had no involvements in any phase of the work.

## Appendix A. Supplementary data

Supplementary data to this article can be found online at https://doi.org/10.1016/j.geoderma.2024.116825.

## References


Arduino, E., Barberis, E., Ajmone Marsan, F., Zanini, E., Franchini, M., 1986. Iron oxides and clay minerals within profiles as indicators of soil age in Northern Italy. Geoderma 37, 45–55. https://doi.org/10.1016/0016-7061(86)90042-X.

Ashworth, J., Keyes, D., Kirk, R., Lessard, R., 2001. Standard procedure in the hydrometer mehod for particle size analysis. Commun. Soil Sci. Plant Anal. 32, 633–642. https://doi.org/10.1081/CSS-100103897.

Bouman, B.A.M., Humphreys, E., Tuong, T.P., Barker, R., 2007. Rice and Water, in: Donald, L.S. (Ed.), Advances in Agronomy. Academic Press, pp. 187–237. doi: 10.1016/S0065-2113(04)92004-4.

Campioli, M., Vicca, S., Luyssaert, S., Bilcke, J., Ceschia, E., Chapin Iii, F.S., Ciais, P., Fernandez-Martinez, M., Malhi, Y., Obersteiner, M., Olefeldt, D., Papale, D., Piao, S. L., Penuelas, J., Sullivan, P.F., Wang, X., Zenone, T., Janssens, I.A., 2015. Biomass production efficiency controlled by management in temperate and boreal ecosystems. Nature Geosci. 8, 843–846. https://doi.org/10.1038/ngeo2553.

Chakrawal, A., Calabrese, S., Herrmann, A.M., Manzoni, S., 2022. Interacting bioenergetic and stoichiometric controls on microbial growth. Front. Microbiol.

Chiti, T., Gardin, L., Perugini, L., Quaratino, R., Vaccari, F.P., Miglietta, F., Valentini, R., 2012. Soil organic carbon stock assessment for the different cropland land uses in Italy. Biol. Fertil. Soils 48, 9–17. https://doi.org/10.1007/s00374-011-0599-4.

Colombo, C., Palumbo, G., He, J.-Z., Pinton, R., Cesco, S., 2014. Review on iron availability in soil: interaction of Fe minerals, plants, and microbes. J. Soil. Sediment. 14, 538–548. https://doi.org/10.1007/s11368-013-0814-z.

Cotrufo, M.F., Lavallee, J.M., 2022. Soil organic matter formation, persistence, and functioning: A synthesis of current understanding to inform its conservation and regeneration, in: Advances in Agronomy. Elsevier, pp. 1–66. doi:10.1016/bs.agron.2021.11.002.

Dunham-Cheatham, S., Zhao, Q., Obrist, D., Yang, Y., 2020. Unexpected mechanism for glucose-primed soil organic carbon mineralization under an anaerobic aerobic transition. Geoderma 376. https://doi.org/10.1016/j.geoderma.2020.114535.

Giannetta, B., de Souza, D., Aquilanti, G., Celi, L., Said-Pullicino, D., 2022. Redox-driven changes in organic C stabilization and Fe mineral transformations in temperate hydromorphic soils. Geoderma 406. https://doi.org/10.1016/j.geoderma.2021.115532.

Golchin, A., Oades, J., Skjemstad, J., Clarke, P., 1994. Study of free and occluded particulate organic matter in soils by solid-state C-13 CP/MAS NMR-spectroscopy and scanning electron microscopy. Aust. J. Soil Res. 32, 285–309. https://doi.org/10.1071/SR9940285.

Grybos, M., Davranche, M., Gruau, G., Petitjean, P., Pédrot, M., 2009. Increasing pH drives organic matter solubilization from wetland soils under reducing conditions. Geoderma 154, 13–19. https://doi.org/10.1016/j.geoderma.2009.09.001.

Hall, S., Berhe, A., Thompson, A., 2018. Order from disorder: do soil organic matter composition and turnover co-vary with iron phase crystallinity? Biogeochemistry 140, 93–110. https://doi.org/10.1007/s10533-018-0476-4.

Huang, W., Hall, S.J., 2017. Elevated moisture stimulates carbon loss from mineral soils by releasing protected organic matter. Nat. Commun. 8, 1774. https://doi.org/10.1038/s41467-017-01998-z.

Huang, X., Kang, W., Guo, J., Wang, L., Tang, H., Li, T., Yu, G., Ran, W., Hong, J., Shen, Q., 2020. Highly reactive nanomineral assembly in soil colloids: Implications for paddy soil carbon storage. Sci. Total Environ. 703 https://doi.org/10.1016/j.scitotenv.2019.134728.

Jackson, R.B., Canadell, J., Ehleringer, J.R., Mooney, H.A., Sala, O.E., Schulze, E.D., 1996. A global analysis of root distributions for terrestrial biomes. Oecologia 108, 389–411.

King, A.E., Amsili, J.P., Córdova, S.C., Culman, S., Fonte, S.J., Kotcon, J., Liebig, M., Masters, M.D., McVay, K., Olk, D.C., Schipanski, M., Schneider, S.K., Stewart, C.E., Cotrufo, M.F., 2023. A soil matrix capacity index to predict mineral-associated but not particulate organic carbon across a range of climate and soil pH. Biogeochemistry 165, 1–14. https://doi.org/10.1007/s10533-023-01066-3.

Kleber, M., Mikutta, R., Torn, M.S., Jahn, R., 2005. Poorly crystalline mineral phases protect organic matter in acid subsoil horizons. Eur. J. Soil Sci. 56, 717–725. https://doi.org/10.1111/j.1365-2389.2005.00706.x.

Kögel-Knabner, I., Amelung, W., Cao, Z.H., Fiedler, S., Frenzel, P., Jahn, R., Kalbitz, K., Kolbl, A., Schloter, M., 2010. Biogeochemistry of paddy soils. Geoderma 157, 1–14. https://doi.org/10.1016/j.geoderma.2010.03.009.

Kölbl, A., Schad, P., Jahn, R., Amelung, W., Bannert, A., Cao, Z., Fiedler, S., Kalbitz, K., Lehndorff, E., Müller-Niggemann, C., Schloter, M., Schwark, L., Vogelsang, V., Wissing, L., Kögel-Knabner, I., 2014. Accelerated soil formation due to paddy management on marshlands (Zhejiang Province, China). Geoderma 228, 67–89. https://doi.org/10.1016/j.geoderma.2013.09.005.

Lavallee, J.M., Soong, J.L., Cotrufo, M.F., 2020. Conceptualizing soil organic matter into particulate and mineral-associated forms to address global change in the 21st century. Glob. Chang. Biol. 26, 261–273. https://doi.org/10.1111/gcb.14859.

Liang, C., Schimel, J.P., Jastrow, J.D., 2017. The importance of anabolism in microbial control over soil carbon storage. Nat. Microbiol. 2, 17105. https://doi.org/10.1038/nmicrobiol.2017.105.

Liu, Y., Ge, T., Zhu, Z., Liu, S., Luo, Y., Li, Y., Wang, P., Gavrichkova, O., Xu, X., Xu, J., Wu, J., Guggenberger, G., Kuzyakov, Y., 2019. Carbon input and allocation by rice into paddy soils: a review. Soil Biol. Biochem. 133, 97–107. https://doi.org/10.1016/j.soilbio.2019.02.019.

Liu, Y., Ge, T., van Groenigen, K.J., Yang, Y., Wang, P., Cheng, K., Zhu, Z., Wang, J., Li, Y., Guggenberger, G., Sardans, J., Penuelas, J., Wu, J., Kuzyakov, Y., 2021. Rice paddy soils are a quantitatively important carbon store according to a global synthesis. Communications Earth & Environment 2, 154. https://doi.org/10.1038/s43247-021-00229-0.

Livsey, J., Kätterer, T., Vico, G., Lyon, S.W., Lindborg, R., Scaini, A., Da, C.T., Manzoni, S., 2019. Do alternative irrigation strategies for rice cultivation decrease water footprints at the cost of long-term soil health? Environ. Res. Lett. 14, 074011 https://doi.org/10.1088/1748-9326/ab2108.

Livsey, J., Thi Da, C., Scaini, A., Lan, T.H.P., Long, T.X., Berg, H., Manzoni, S., 2021. Floods, soil and food – interactions between water management and rice production within an Giang province Vietnam. Agriculture, Ecosystems & Environment 320, 107589. https://doi.org/10.1016/j.agee.2021.107589.

Lugato, E., Lavallee, J.M., Haddix, M.L., Panagos, P., Cotrufo, M.F., 2021. Different climate sensitivity of particulate and mineral-associated soil organic matter. Nat. Geosci. 14, 295–300. https://doi.org/10.1038/s41561-021-00744-x.

Ma, Y., Woolf, D., Fan, M., Qiao, L., Li, R., Lehmann, J., 2023. Global crop production increase by soil organic carbon. Nat. Geosci. https://doi.org/10.1038/s41561-023-01302-3.

McNaught, A.D., Wilkinson, A., 1997. IUPAC Compendium of Chemical Terminology, 2nd ed. Blackwell Scientific Publications, Oxford, UK.

Mehra, O.P., Jackson, M.L., 1960. Iron oxide removal from soils and clay by a dithionite-citrate system buffered with sodium bicarbonate. Clay Clay Miner. 7, 317–327.

Messing, I., Alriksson, A., Johansson, W., 1997. Soil physical properties of afforested and arable land. Soil Use Manag. 13, 209–217. https://doi.org/10.1111/j.1475-2743.1997.tb00588.x.

Mikutta, R., Lorenz, D., Guggenberger, G., Haumaier, L., Freund, A., 2014. Properties and reactivity of Fe-organic matter associations formed by coprecipitation versus adsorption: clues from arsenate batch adsorption. Geochim. Cosmochim. Acta 144, 258–276. https://doi.org/10.1016/j.gca.2014.08.026.

Moretti, B., Bertora, C., Grignani, C., Lerda, C., Celi, L., Sacco, D., 2020. Conversion from mineral fertilisation to MSW compost use: nitrogen fertiliser value in continuous maize and test on crop rotation. Sci. Total Environ. 705 https://doi.org/10.1016/j.scitotenv.2019.135308.

Nolè, A., Collalti, A., Borghetti, M., Chiesi, M., Chirici, G., Magnani, F., Marras, S., Maselli, F., Sirca, C., Spano, D., Valentini, R., 2015. The Role of Managed Forest Ecosystems: A Modeling Based Approach, in: Valentini, R., Miglietta, F. (Eds.), The Greenhouse Gas Balance of Italy: An Insight on Managed and Natural Terrestrial Ecosystems. Springer Berlin Heidelberg, Berlin, Heidelberg, pp. 71–85. doi:10.1007/978-3-642-32424-6_5.

Pan, G., Smith, P., Pan, W., 2009. The role of soil organic matter in maintaining the productivity and yield stability of cereals in China. Agr. Ecosyst. Environ. 129, 344–348. https://doi.org/10.1016/j.agee.2008.10.008.

Rasmussen, C., Heckman, K., Wieder, W.R., Keiluweit, M., Lawrence, C.R., Berhe, A.A., Blankinship, J.C., Crow, S.E., Druhan, J.L., Hicks Pries, C.E., Marin-Spiotta, E., Plante, A.F., Schädel, C., Schimel, J.P., Sierra, C.A., Thompson, A., Wagai, R., 2018. Beyond clay: towards an improved set of variables for predicting soil organic matter content. Biogeochemistry 137, 297–306. https://doi.org/10.1007/s10533-018-0424-3.

Regione Piemonte, 2022. Soil Map 1:50000. https://www.geoportale.piemonte.it/geonetwork/srv/eng/catalog.search#/metadata/r_piemon:37c6413b-b07f-4f4c-9344-f2e43ea52bbd.

Said-Pullicino, D., Miniotti, E., Sodano, M., Bertora, C., Lerda, C., Chiaradia, E., Romani, M., Cesari de Maria, S., Sacco, D., Celi, L., 2016. Linking dissolved organic carbon cycling to organic carbon fluxes in rice paddies under different water management practices. Plant and Soil 401, 273–290. https://doi.org/10.1007/s11104-015-2751-7.

Said-Pullicino, D., Giannetta, B., Demeglio, B., Missong, A., Gottselig, N., Romani, M., Bol, R., Klumpp, E., Celi, L., 2021. Redox-driven changes in water-dispersible colloids and their role in carbon cycling in hydromorphic soils. Geoderma 385. https://doi.org/10.1016/j.geoderma.2020.114894.

Šantrůčková, H., Picek, T., Tykva, R., Šimek, M., Pavlů, B., 2004. Short-term partitioning of C-14- U -glucose in the soil microbial pool under varied aeration status. Biol. Fertil. Soils 40, 386–392. https://doi.org/10.1007/s00374-004-0790-y.

Schmidt, M., Rumpel, C., Kogel-Knabner, I., 1999. Evaluation of an ultrasonic dispersion procedure to isolate primary organomineral complexes from soils. Eur. J. Soil Sci. 50, 87–94. https://doi.org/10.1046/j.1365-2389.1999.00211.x.

Schwertmann, U., 1964. Differenzierung der Eisenoxide des Bodens durch Extraktion mit Ammoniumoxalat-Lösung. Z. Pflanzenarnähr. Düng Bodenk. 105, 194–202.

Sever, M., Alberti, G., Delle Vedove, G., Marjanovic, H., 2019. Temporal evolution of carbon stocks, fluxes and carbon balance in pedunculate oak chronosequence under close-to-nature forest management. Forests 10. https://doi.org/10.3390/f10090814.

Sodano, M., Lerda, C., Nistico, R., Martin, M., Magnacca, G., Celi, L., Said-Pullicino, D., 2017. Dissolved organic carbon retention by coprecipitation during the oxidation of ferrous iron. Geoderma 307, 19–29. https://doi.org/10.1016/j.geoderma.2017.07.022.

Sohi, S., Mahieu, N., Arah, J., Powlson, D., Madari, B., Gaunt, J., 2001. A procedure for isolating soil organic matter fractions suitable for modeling. Soil Sci. Soc. Am. J. 65, 1121–1128. https://doi.org/10.2136/sssaj2001.6541121x.

Szalai, Z., Ringer, M., Németh, T., Sipos, P., Perényi, K., Pekker, P., Balázs, R., Vancsik, A., Zacháry, D., Szabó, L., Filep, T., Varga, G., Jakab, G., 2021. Accelerated soil development due to seasonal water-saturation under hydric conditions. Geoderma 401. https://doi.org/10.1016/j.geoderma.2021.115328.

The MathWorks Inc., 2018. MATLAB version: 9.5.0.944444 (R2018b). The MathWorks Inc., Natick, Massachusetts. https://www.mathworks.com.

von Luetzow, M., Kogel-Knabner, I., Ludwig, B., Matzner, E., Flessa, H., Ekschmitt, K., Guggenberger, G., Marschner, B., Kalbitz, K., 2008. Stabilization mechanisms of organic matter in four temperate soils: Development and application of a conceptual model. Journal of Plant Nutrition and Soil Science-Zeitschrift Fur Pflanzenernahrung Und Bodenkunde 171, 111–124.

Wiesmeier, M., Urbanski, L., Hobley, E., Lang, B., von Lutzow, M., Marin-Spiotta, E., van Wesemael, B., Rabot, E., Liess, M., Garcia-Franco, N., Wollschlager, U., Vogel, H.J., Kogel-Knabner, I., 2019. Soil organic carbon storage as a key function of soils - a review of drivers and indicators at various scales. Geoderma 333, 149–162. https://doi.org/10.1016/j.geoderma.2018.07.026.

Winkler, P., Kaiser, K., Jahn, R., Mikutta, R., Fiedler, S., Cerli, C., Kölbl, A., Schulz, S., Jankowska, M., Schloter, M., Müller-Niggemann, C., Schwark, L., Woche, S.K., Kümmel, S., Utami, S.R., Kalbitz, K., 2019. Tracing organic carbon and microbial community structure in mineralogically different soils exposed to redox fluctuations. Biogeochemistry 143, 31–54. https://doi.org/10.1007/s10533-019-00548-7.

Wu, J., 2011. Carbon accumulation in paddy ecosystems in subtropical China: evidence from landscape studies. Eur. J. Soil Sci. 62, 29–34. https://doi.org/10.1111/j.1365-2389.2010.01325.x.